NASA TM X-269

TECHNICAL MEMORANDUM
X-269

AERODYNAMIC AND LANDING MEASUREMENTS

OBTAINED DURING THE FIRST POWERED FLIGHT OF THE

NORTH AMERICAN X-15 RESEARCH AIRPLANE

By NASA Flight Research Center

Flight Research Center
Edwards, Calif.

NATIONAL AERONAUTICS AND SPACE ADMINISTRATION

WASHINGTON

January 1960
Declassified April 12, 1961

NATIONAL AERONAUTICS AND SPACE ADMINISTRATION

TECHNICAL MEMORANDUM X-269

AERODYNAMIC AND LANDING MEASUREMENTS OBTAINED DURING THE FIRST POWERED FLIGHT OF THE NORTH AMERICAN X-15 RESEARCH AIRPLANE

By NASA Flight Research Center

SUMMARY

During the first powered flight of the North American X-15 research airplane on September 17, 1959, a Mach number of 2.1 and an altitude of 52,000 feet were attained. Static and dynamic maneuvers were performed to evaluate the characteristics of the airplane at subsonic and supersonic speeds. Data from these maneuvers as well as from the launch and landing phases are presented, discussed, and compared with predicted values.

The rate of separation of the X-15 from the B-52 carrier airplane at launch was less than that predicted by wind-tunnel studies and was less rapid than in the lightweight condition of the initial glide flight. In addition, the angular motions and bank angle attained following the launch were of lesser magnitude than in the glide flight.

Stable longitudinal-stability trends were apparent during the acceleration to maximum speed, and the pilot reported experiencing little or no transonic trim excursions. An inexplicable high-frequency vibration, which occurred at Mach numbers above 1.4, is being investigated further.

Essentially linear lift and stability characteristics were indicated within the limited ranges of angle of attack and angle of sideslip investigated. The dynamic longitudinal and lateral-directional stability and control-effectiveness characteristics appeared satisfactory to the pilot. Although the longitudinal- and lateral-directional-damping ratios showed no significant change from subsonic to supersonic speeds, on the basis of time to damp, the damping characteristics at supersonic speeds appeared to the pilot to be somewhat improved over those at subsonic speeds.

The subsonic flight-determined boundary for onset of buffet is defined by an airplane normal-force coefficient which decreased from a value of 0.6 at a Mach number of 0.6 to a minimum value of 0.4 at a Mach number of 0.8. No buffet was experienced above a Mach number of 0.95.

The approach and landing characteristics appeared satisfactory and no control problems were reported by the pilot. The use of the center control stick, availability of augmented pitch damping, and the absence of significant flap-trim change which accompanied a slow rate of flap deflection tended to avert the pitching oscillations experienced during the initial glide flight of the X-15. This combination of conditions made the landing of the powered flight more satisfactory.

Vertical velocities of 5 feet per second and 15 feet per second encountered during main-gear and nose-gear touchdown, respectively, were less than design values. At nose-gear impact, the main-gear shock-strut deflection was increased to full travel and the design shock-strut force was exceeded by 7,000 pounds for the right main gear and 6,000 pounds for the left main gear.

INTRODUCTION

The X-15 airplane was designed and constructed by North American Aviation, Inc., under the technical direction of the National Aeronautics and Space Administration and the cooperative efforts of the U.S. Air Force and the U.S. Navy, for hypersonic flight research. The airplane is currently undergoing initial demonstration tests by the manufacturer at Edwards Air Force Base, Calif. Because of the large speed and altitude range for which the X-15 was designed, various aerodynamic and structural features and compromises were necessary which require flight checkout prior to enlarging the flight-performance envelope. The first flight of the airplane, which was launched unpowered in a propellants-empty condition to enable the pilot to concentrate on the launch and landing characteristics and on systems operation, is reported in reference 1. Details of the performance of the unique landing-gear configuration of the X-15 during this first flight are reported in reference 2.

This paper presents some of the results from the first powered flight of the X-15, which was conducted to a Mach number of about 2.1 and to an altitude of about 52,000 feet. Data obtained during launch in the normal fueled condition for powered flight, during the subsequent subsonic and supersonic maneuvering, and during the approach and landing are presented and compared with design and predicted characteristics and also with results obtained during the first flight.

SYMBOLS

a_n	normal acceleration at center of gravity, g units
a_v	left-main-gear normal acceleration, g units
C_l	rolling-moment coefficient
C_{l_β}	effective dihedral derivative, per deg
$C_{l_{\delta_a}}$	aileron-effectiveness derivative, $\frac{dC_l}{d\delta_a}$, per deg
$C_{l_{\delta_v}}$	rate of change of rolling-moment coefficient with respect to vertical-tail deflection, per deg
C_m	pitching-moment coefficient
C_{m_α}	longitudinal stability derivative, per deg
$C_{m_{\delta_h}}$	horizontal-tail-effectiveness derivative, $\frac{dC_m}{d\delta_h}$, per deg
C_N	airplane normal-force coefficient
C_{N_α}	normal-force-curve slope, per deg
C_n	yawing-moment coefficient
C_{n_β}	directional stability derivative, per deg
$C_{n_{\delta_v}}$	vertical-tail-effectiveness derivative, $\frac{dC_n}{d\delta_v}$, per deg
C_Y	airplane side-force coefficient
F_s	main-gear shock-strut force, lb
F_v	pedal force, lb
g	acceleration due to gravity, ft/sec^2
h	geometric altitude, ft

h'	altitude above reference plane, ft
h_p	pressure altitude, ft
I_X	moment of inertia about X-axis, slug-ft^2
I_Y	moment of inertia about Y-axis, slug-ft^2
I_Z	moment of inertia about Z-axis, slug-ft^2
I_{XZ}	product of inertia, $1/2(I_Z - I_X)\sin 2\epsilon$, slug-ft^2
L_h	aerodynamic load on horizontal tail perpendicular to X-Y plane, lb
M	Mach number
P	period of longitudinal or lateral-directional oscillation, sec
p	rolling velocity, deg/sec
q	pitching velocity, deg/sec
r	yawing velocity, deg/sec
S	wing area, sq ft
$T_{1/2}$	time required for absolute value of transient oscillation to damp to half amplitude, sec
t	time, sec
V_i	indicated airspeed, knots
V_T	true velocity, knots
V_v	vertical velocity, ft/sec
W	airplane weight, lb
Z	separation distance between X-15 and B-52, ft
α	angle of attack of airplane center line, deg
β	angle of sideslip, deg

δ_a	total aileron deflection, $\delta_{h_L} - \delta_{h_R}$, deg
δ_f	flap deflection, deg
δ_h	horizontal-tail deflection, $\frac{\delta_{h_L} + \delta_{h_R}}{2}$, deg
δ_s	main-gear shock-strut deflection, in.
δ_v	vertical-tail deflection, deg
ϵ	angle between airplane body X-axis and principal X-axis, deg
ξ	ratio of actual damping to critical damping
θ	pitch attitude, deg
φ	bank attitude, deg

Subscripts:

L	left
R	right

AIRPLANE

The X-15 airplane (figs. 1 and 2) is a single-place experimental research aircraft designed to explore the flight regime at hypersonic speeds up to 6,600 feet per second and at altitudes to at least 250,000 feet. The airplane is carried aloft under the right wing of a B-52 carrier aircraft and is launched at an altitude of about 38,000 feet, after which it performs its powered flight mission and glides to a landing.

All aerodynamic control surfaces of the X-15 are actuated by irreversible hydraulic systems. Longitudinal control is provided by deflection of the all-movable horizontal tail; lateral control is provided by differential deflection of the left and right portions of the horizontal tail. The movable portions of the upper and lower wedge-sectioned vertical tails provide directional control, and the lower movable section (indicated by the dashed line in fig. 1) is jettisoned prior to landing for proper ground clearance. Speed brakes are located on the rear fixed portion of the upper and lower vertical tails. Auxiliary damping is provided about all three axes in a conventional manner along with a "yar" damper which provides a crossfeed

of the yaw-rate signal into the roll damper. The landing gear consists of a corotating dual-wheel nose gear located well forward and a main gear equipped with steel skids (fig. 3) located under the tail. Pertinent physical characteristics of the airplane are presented in table I. Additional details pertinent to the airplane and the landing-gear system are presented in references 1 and 2.

The airplane used for the first powered flight was the number 2 airplane of this series and is basically similar to the number 1 airplane used in the initial unpowered flight (refs. 1 and 2). As a result of the experience gained in the glide flight, the manufacturer included the following modifications in the number 2 airplane prior to the subject flight: the stabilizer-deflection rate was increased from 15 degrees per second to 25 degrees per second; the longitudinal-force gradient was increased approximately 30 percent; the longitudinal breakout force was increased slightly; and the main-gear shock-strut pressure was increased. The X-15 is currently equipped with two XLR-11 interim rocket motors, manufactured by the Reaction Motors Division of the Thiokol Chemical Corp., which are mounted one above the other in the vertical plane in the rear end of the fuselage. Each rocket motor has four individually controlled cylinders which utilize an alcohol-water mixture as the fuel and liquid oxygen as the oxidizer. The combined sea-level thrust of both motors is approximately 13,000 pounds.

INSTRUMENTATION

The following quantities pertinent to this investigation were recorded on NASA internal-recording instruments which were synchronized by a common timer:

Airspeed and pressure altitude

Normal and transverse acceleration at airplane center of gravity

Rolling, yawing, and pitching velocity and acceleration

Vertical accelerations of airplane directly above right main gear and nose gear

Main-landing-gear shock-strut load and deflection

Horizontal-tail load

Right-wing bending stress

Angle of attack and angle of sideslip

Aileron, vertical-tail, horizontal-tail, and flap deflection

Pedal force

The airspeed and pressure altitude were measured with an NASA pitot-static tube mounted on the end of the nose boom. Free-floating vanes also mounted on the nose boom were used to measure angle of attack and angle of sideslip. The angles presented were not corrected for errors induced by aircraft pitching, yawing, or rolling motions. The angular velocities were referenced to the airplane body axis. Angles of bank and pitch were obtained by integrating the respective records of rolling and pitching velocity.

Complete photo coverage was obtained by using ground-support equipment as a means of determining airplane space-positioning data from launch, and during the approach, landing, and runout phases of the flight. Askania Cine-Theodolite cameras, operated by personnel of the Air Force Flight Test Center, and an Air Force Missile Test Center Model II tracking radar furnished space-positioning data in flight. For more precise position data and rates of sink near ground level and through touchdown and final landing runout, AFFTC-operated Akeley phototheodolite cameras were used. Photographic coverage by North American Aviation also aided in the analysis of this X-15 flight.

TEST CONDITIONS

At launch from the B-52 carrier aircraft, the X-15 airplane weighed 32,700 pounds with a center-of-gravity position of 20 1/2 percent of the mean aerodynamic chord. The auxiliary damper system was operating for all modes and remained in operation throughout the flight. The use of oxidizer and fuel caused a continued rearward movement of the center of gravity to about 22 1/2 percent of the mean aerodynamic chord during the powered portion of the flight, and subsequent fuel jettison moved the center of gravity forward to about 21 percent of the mean aerodynamic chord. In the landing pattern, jettison of the ventral fin reduced the weight of the airplane about 170 pounds. This effect, plus the extension of flap and gear for landing, provided touchdown conditions of an airplane weight of 14,000 pounds and a center of gravity at about 19 1/2 percent of the mean aerodynamic chord.

PRESENTATION OF RESULTS

Data obtained during the various phases of the flight, from launch to the landing runout, are presented in the following figures:

	Figures
General flight plan	4
Time history of the launch	5
Trim characteristics during acceleration run	6
Static longitudinal-stability characteristics	7, 8
Boundary for onset of buffet	9
Static lateral-directional-stability characteristics	10
Approach and landing characteristics	11
Landing runout characteristics	12 to 17

DISCUSSION

General Flight Plan

The geographical path over the ground, with respect to Rogers and Rosamond Dry Lakes, which was traversed by the X-15 during its first powered flight is shown in figure 4. Because of the limited gliding capability of the X-15, the launch and the subsequent maneuvering flight were performed in the proximity of the intended landing area to provide a margin of safety in the event of engine malfunction.

As indicated by the flight plan of figure 4, the launch occurred approximately 13 nautical miles southwest of Rogers Dry Lake on a northeast heading. About 4 seconds after drop, while performing recovery from the launch, the pilot initiated operation of the rocket engine. Within 12 seconds after launch, all 8 cylinders were operating. During the launch recovery, the pilot doubled the roll-damper gain in order to decrease the apparent sensitivity in roll. This higher damper gain was used throughout the remainder of the flight. Inasmuch as all dampers were operating throughout the flight, all control-deflection data presented in this paper are net deflections resulting from both pilot and damper inputs. During the supersonic climb and acceleration which followed launch recovery, pitch, roll, and yaw pulses were performed and a pushover to 0.5g was initiated to attain near-level flight. After a turn to a southeast heading was accomplished with the altitude continuing to increase to a peak of 52,000 feet, the airplane continued to accelerate and additional control pulses were performed. The peak Mach number of 2.1 was attained at engine burnout with the airplane in a very slight dive, and was followed by an eastward turn back to base.

Speed decreased rapidly following the burnout and turn to base, and at subsonic speeds, additional pulses and a sideslip maneuver were performed. For the approach and landing, an S-shaped pattern, similar to that flown on the glide flight, was performed. The lower movable vertical tail was jettisoned during the turn into final approach at an altitude of about 3,000 feet above the dry lakebed, and flap extension was initiated at a geometric altitude of about 300 feet. Because of a malfunction, however, the flaps were not fully extended until 11 seconds after touchdown. The gear was extended at a geometric altitude of about 250 feet while the flare was being completed, and the landing and rollout followed on the lakebed of Rogers Dry Lake.

Although the side-located control stick was used during the launch and during almost the entire period of supersonic flight, the center stick was utilized during the subsonic maneuvering following engine burnout and during the approach and landing.

Launch Characteristics

From an analysis of internal X-15 instrumentation and from motion pictures taken from a rearward position on the B-52 carrier airplane, a time history of the pertinent quantities measured during launch was prepared. These data are presented in figure 5. At launch, the horizontal tail was set at an airplane nose-up attitude of 1 1/2° and the ailerons were set for a left roll of 3°; the abrupt control motions following launch resulted primarily from pilot input for the longitudinal control and primarily from damper input for the lateral control. Also, following launch, the normal acceleration decreased rapidly to slightly less than 0g and right-roll velocity increased abruptly to over 30 degrees per second. After 0.4 second the vertical separation of the X-15 from the B-52 was about 2.5 feet and the X-15 vertical tail cleared the B-52 wing cutout by about 1 foot. About 0.7 second following launch, the vertical separation of the X-15 from the B-52 was about 5 feet and bank angle had almost reached its peak value of about 18°. The X-15 was essentially stabilized at 0.5g within 3 seconds after launch, and the pilot initiated rocket-engine operation about 1 second later. The pilot reported that to expedite initiation of engine operation he had not attempted to stabilize at any specific level of normal acceleration, which explains the stabilization level of 0.5g. Throughout the launch maneuver, airspeed was essentially constant and the pitching and yawing motions were small. The altitude lost before stabilization at approximately 0.5g was about 200 feet, but about 4,000 feet were lost before the pilot initiated the climb to altitude.

A comparison of the present heavyweight launch with the lightweight launch of reference 1 indicated some apparent differences. The most

noticeable differences observed by the pilot were the less rapid buildup of rolling velocity and pitching velocity and the slower separation rate of the X-15 from the B-52 for the heavyweight condition. In addition, the bank angle attained in the heavyweight launch was appreciably less than that recorded in the lightweight condition.

A comparison of the flight data with the wind-tunnel data of reference 3 indicates a lower rate of separation in flight of the X-15 from the B-52 airplane. This effect can be attributed to the fact that zero stabilizer-trim setting was used in the wind-tunnel studies, in contrast to the airplane nose-up trim deflections shown in figure 5 for flight. However, the flight-test data show somewhat greater rolling and pitching rates at separation than are shown by the comparative wind-tunnel data.

Climb and Acceleration Characteristics

Flight-control characteristics.- During the climb and acceleration on a northeast heading following the launch, various maneuvers were performed which are discussed and analyzed in other sections of this paper. Although the rate of performance and the accompanying altitude changes of these maneuvers obviated the presentation of significant data for the trim characteristics over the transonic and low supersonic range covered up to $M \approx 1.6$, some intelligible results were apparent. Little or no transonic trim excursions were apparent to the pilot or shown by the data. With normal roll-damper gain, the pilot found the airplane sensitive in roll with both the center control stick and the side-located control stick; however, some improvement was noted when the roll gain was doubled. Although various maneuvers were performed during the acceleration on a southwest heading, as previously discussed, some evaluation and presentation of significant trim data were feasible. Pertinent quantities measured during the powered acceleration run are presented in figure 6 as a function of Mach number from $M = 1.6$ to $M = 2.1$. The altitude at this point in the flight was reasonably constant ($h_p \approx 50{,}000$ ft), however the airplane wing loading varied from about $W/S = 102.0$ pounds per square foot to $W/S = 91.5$ pounds per square foot during the run. For continuity of the data, the limited regions of control maneuvering and aircraft response were faired and are shown in the figure by short dashed lines. Stable longitudinal trends are indicated, particularly considering that the initial portion of the run was made at less than 1 g trim. Measured angle of attack and stabilizer angle required for trim were within 1° of predicted values. It may be noted that a slight directional out-of-trim moment was measured, resulting in less than 1° of left sideslip. The right-rudder and left-aileron control used throughout the acceleration would tend to maintain this left sideslip. The reason for this sideslipping trend is not known at this time.

Airplane vibration.- During the climb and acceleration, a high-frequency vibration of the airplane started at a Mach number of 1.4 and an altitude of 49,000 feet and persisted until the airplane had attained peak Mach number and altitude and had decelerated to a Mach number of 1.38 and an altitude of 46,500 feet. The vibration was felt or sensed by the pilot. The frequency of the vibration, as measured by a strain gage at the right-wing root, was a nominal 110 cycles per second which is approximately the frequency for the second mode of wing torsion. The stress level of the wing-bending vibration reached a maximum level of about 500 pounds per square inch. The vibration was additionally detected by high-frequency accelerometers in the fuselage at the nose, center of gravity, and tail. At the center of gravity the maximum amplitude of the vibration was of the order of ±1.5g. Although the source of this vibration is not presently known, both mechanical and aerodynamic sources are being investigated.

Longitudinal Characteristics

Dynamic longitudinal stability and control.- Data obtained from the longitudinal-control pulses and other flight data qualitatively indicated satisfactory damping characteristics. Although several pulse maneuvers were performed to evaluate dynamic characteristics, only two were considered suitable for preliminary quantitative analysis (table II). The sparsity of flight data currently available precludes any comparison with wind-tunnel results until a more complete analysis of flight data can be performed. Within the limited Mach number range for which the flight data could be analyzed, there appeared to be little change in damping; however, the pilot reported that somewhat more damping prevailed at supersonic speeds than at subsonic speeds and the airplane appeared to be very stable. As might be expected, the use of the pitch damper materially improved the damping characteristics of the airplane as compared with the characteristics exhibited during the glide flight.

Static longitudinal stability.- Time histories of quantities measured during reasonably constant speed and altitude turn maneuvers at $M = 1.56$ and $h_p = 48{,}000$ feet, and at $M = 2.00$ and $h_p = 47{,}000$ feet are presented in figure 7. Control-force data for these maneuvers were not available. An incremental normal acceleration of approximately 2g was attained in each maneuver, and positive longitudinal stability trends are noted over the lift range covered. A small-amplitude porpoising motion is shown for both maneuvers and may indicate the desirability of using higher values of pitch-damper gain.

Longitudinal-stability crossplots for these maneuvers are presented in figure 8 and show fairly linear variations of the stability

measurements and normal-force-curve slopes. No reduction in stability with increase in lift is indicated from either the variation of stabilizer position with angle of attack or with lift; these variations indicate adequate static stick-fixed stability levels at $M = 1.56$ and $M = 2.00$. In addition, the level of apparent stability increased slightly with this increase in Mach number.

A comparison of the flight data with results obtained from the manufacturer's estimates indicates generally good agreement in the variation of trimmed C_N with α and in the variation of δ_h with C_N. Reasons for differences in absolute values of the flight and estimated data are not apparent at present.

Buffet boundary.- The boundary for onset of buffet, as determined from the first two flights of the X-15 airplane, is shown in figure 9 to be defined by an airplane normal-force coefficient which decreased from a value of 0.6 at $M = 0.6$ to a minimum value of 0.4 at $M = 0.8$. No buffet was experienced above a Mach number of 0.95. Buffet magnitudes at launch were negligible as a result of the rapid decrease in normal acceleration to 0g followed by stabilization at 0.5g. The subsonic buffet boundary for the airplane is essentially the same as estimated from wind-tunnel wing lift-break data and from other airplanes of similar configuration. Although the low supersonic speed range was not completely evaluated for buffeting, no buffet was noted at values of C_N up to 0.82 at $M = 1.5$.

Lateral-Directional Characteristics

Dynamic lateral stability and control.- Results of the analysis of the directional-control pulses made during the flight are shown in table III, as obtained from approximate equations. The values of the oscillation period are in close agreement with those obtained from unpublished analog studies. The values of P and $T_{1/2}$ indicate stability and damping characteristics, with dampers operating, which were considered satisfactory by the pilot. The pilot commented that the damping at supersonic speeds was somewhat improved over that at subsonic speeds, which is verified by the values of $T_{1/2}$ shown; however, the values of damping ratio shown are approximately the same at all speeds tested. The pilot also reported very little rolling response due to rudder input and small yawing motions due to aileron inputs.

The values of the vertical-tail-effectiveness derivative $C_{n_{\delta_v}}$ exhibited only moderate changes over the speed range tested; however, successful determination of $C_{l_{\delta_v}}$ from flight data was precluded by

the inputs of the roll control by the damper system. A study of the three aileron pulses performed indicated some questionable characteristics in the free-oscillation portions of the maneuvers, thus only the roll-control-effectiveness derivative $C_{l_{\delta_a}}$ was determined. The results, shown in table IV, indicate an anticipated decrease in the roll-control-effectiveness derivative with increase in Mach number. As noted in the preceding discussion of longitudinal dynamic data, the sparsity of lateral-directional dynamic flight data precludes any comparison with wind-tunnel results until a more complete analysis of flight data can be performed.

Static lateral-directional stability.- Pertinent quantities measured during a sideslip maneuver at $M = 0.95$ and $h_p = 43{,}000$ feet are shown plotted as a function of sideslip angle in figure 10. The sideslip appeared oscillatory in nature, but little or no dihedral effect is apparent from the data and the directional stability and side-force characteristics were positive and almost linear. It appears that full deflection of the vertical tail (7.5°) would produce about 5° of sideslip, which is within 1° higher than predicted. The pilot reported that the rudder power at small deflections appeared to be high as a result of easily developed high side force. He also reported that no dihedral or adverse yaw were apparent.

Landing Characteristics

Approach and touchdown.- Because of the unexpected control problem presented by the oscillations which occurred during the flare portion of the first X-15 landing, considerable attention was focused on the landing phase of the powered flight. In the powered flight, the pilot elected to fly an S-shaped approach pattern similar to that of the glide flight (ref. 1). At a geometric altitude of about 10,000 feet (referenced to the touchdown altitude), a 45°-bank, left turn was initiated. This turn was maintained to an altitude of 1,500 feet at which time the pilot rolled out of the turn into the final approach. While still in the turn, the movable portion of the lower vertical tail was jettisoned as the X-15 passed through an altitude of 3,000 feet.

A time history of the final approach, flare, and touchdown is shown in figure 11. From an approach speed of about 240 knots indicated airspeed and an altitude of slightly over 500 feet, the flare was initiated about 15 seconds prior to touchdown. Rate of sink at this point was about 65 feet per second. The nose and main gear were extended at 230 KIAS about 11 seconds before touchdown at an altitude slightly over 250 feet and with a rate of sink of about 65 fps. Flap deflection was initiated almost 12 seconds prior to touchdown and the flaps started down at a normal rate. About 2 seconds later, however,

the rate changed abruptly and a flap deflection of only 23° had been realized by touchdown. Full deflection was delayed until 11 seconds following touchdown. As shown in figure 11, about 6 seconds before touchdown at an altitude of 100 feet, sink rate was reduced to about 25 feet per second and was further reduced to about 10 feet per second 2 seconds before touchdown at an altitude of 10 feet. Touchdown was performed on the north-south lakebed runway of Rogers Dry Lake at a forward velocity of 184 KIAS, an angle of attack of about 8°, and a rate of sink of about 5 feet per second; winds were from the southwest at 8 to 10 knots.

In contrast to the flare of the glide flight, no major oscillations were experienced during the flare of the powered flight. Some small oscillations in angle of attack (±2°) were noticeable about the time of gear extension, but they were quickly damped. A peak value of 1.65g was evidenced during the flare, but the average level of normal acceleration was only about 1.25g. The pilot reported no landing control problems, and indicated that the higher lift-drag ratio and absence of flap-trim change due to one-half flap deployment produced significant improvements in the control prior to touchdown. Although it is believed that the sensitivity of the side-located control stick used, as well as the absence of pitch-damping augmentation, contributed to the pitching motions experienced prior to landing during the glide flight, the pilot believed that use of the center stick in the powered flight did not improve the landing control characteristics. Operation of the pitch-augmentation system throughout the approach and landing provided the expected improvement in apparent longitudinal characteristics.

Runout.- Skid-mark measurements at touchdown are shown in figure 12, and photographs of the skid marks are shown in figures 13 and 14. As discussed in the preceding section, touchdown was accomplished on the north-south lakebed runway (runway 35) of Rogers Dry Lake at a forward velocity of 184 KIAS and an angle of attack of about 8°, with winds from the southwest at 8 to 10 knots. The airplane first contacted the lakebed on the left main gear, with the outboard trailing edge of the skid scratching the surface for a distance of 11.65 feet, then lifting off. The right main skid then contacted the lakebed 12 feet down the runway from the initial touchdown point of the left main skid, with the outboard trailing edge of the right skid scratching the lakebed for a distance of 2.54 feet before lifting off. The second touchdown, the point at which the gear solidly contacted the ground, was made 39.46 feet for the left skid and 54.25 feet for the right skid from the initial touchdown point of the left main skid. The left and right main skids then left the ground at a distance of 120 and 134 feet, respectively, down the runway from the initial touchdown point. Final touchdown for both the left and right main skids was made 169 feet from the initial touchdown point. The nose-gear touchdown occurred at a point 330 feet down the runway from

the initial touchdown point, and, as seen in figure 12, the nose gear rebounded clear of the ground for 1.2 feet down the runway after initial nose-gear contact. Total runout of the landing was 5,560 feet.

Pertinent quantities measured during the landing are presented in figures 15 to 17 as a variation with time from initial skid contact. It should be noted that because of the cross wind from the left of the airplane, a left sideslip of about 2° was maintained prior to and at touchdown with an accompanying bank angle of nearly 0°. From the data (fig. 16) it can be seen that the maximum deflection for both the right- and left-main-gear shock struts followed the nose-gear impact and the main-gear shock-strut deflection increased from 0.7 inch to 2.58 inches. The resulting shock-strut force (fig. 16) for this maximum condition was 36,000 pounds for the left gear and 37,000 pounds for the right gear, as compared with a design load of 30,000 pounds. The horizontal-tail aerodynamic load (fig. 16), obtained from a preliminary calibration, increased from a value of 1,000 pounds at initial main-gear touchdown to 6,400 pounds at the time of nose-gear impact. Although the initial main-gear touchdown (at which point the skids barely scratched the lakebed surface) occurred at a vertical velocity of 5 feet per second as compared to a main-gear design vertical velocity of 9.0 feet per second, upon second touchdown of the airplane, when the skids solidly contacted the lakebed surface, the left main skid had a vertical velocity of only 4.2 feet per second. The vertical velocity of the nose gear at nose-gear touchdown was 15 feet per second as compared with a design value of 18 feet per second.

An analysis of the skid marks on the lakebed resulting from the landing indicated satisfactory directional-stability characteristics of the skids, with little or no cocking tendency during the touchdown and runout phase of the landing. In addition, during this phase no nosewheel shimmy was observed.

CONCLUSIONS

The first powered flight of the X-15 research airplane, performed up to a Mach number of 2.1 and an altitude of 52,000 feet, led to the following conclusions.

1. The rate of separation of the X-15 from the B-52 carrier airplane at launch was less than that predicted by wind-tunnel studies and was less rapid than in the lightweight condition of the initial glide flight. In addition, the angular motions and bank angle attained following the launch were of lesser magnitude than in the glide flight.

2. Stable longitudinal-stability trends were apparent during the acceleration to maximum speed, and the pilot reported experiencing little or no transonic trim excursions. An inexplicable high-frequency vibration, which occurred at Mach numbers above 1.4, is being investigated further.

3. Essentially linear lift and stability characteristics were indicated within the limited ranges of angle of attack and angle of sideslip investigated. The dynamic longitudinal and lateral-directional stability and control-effectiveness characteristics appeared satisfactory to the pilot. Although the longitudinal- and lateral-directional damping ratios showed no significant change from subsonic to supersonic speeds, on the basis of time to damp, the damping characteristics at supersonic speeds appeared to the pilot to be somewhat improved over those at subsonic speeds.

4. The subsonic flight-determined boundary for onset of buffet is defined by an airplane normal-force coefficient which decreased from a value of 0.6 at a Mach number of 0.6 to a minimum value of 0.4 at a Mach number of 0.8. No buffet was experienced above a Mach number of 0.95.

5. The approach and landing characteristics appeared satisfactory and no control problems were reported by the pilot. The use of the center control stick, availability of augmented pitch damping, and the absence of significant flap-trim change which accompanied a slow rate of flap deflection tended to avert the pitching oscillations experienced during the initial glide flight of the X-15. This combination of conditions made the landing of the powered flight more satisfactory.

6. Vertical velocities of 5 feet per second and 15 feet per second encountered during main-gear and nose-gear touchdown, respectively, were less than design values. At nose-gear impact, the main-gear shock-strut deflection was increased to full travel and the design shock-strut force was exceeded by 7,000 pounds for the right main gear and 6,000 pounds for the left main gear.

Flight Research Center,
National Aeronautics and Space Administration,
Edwards, Calif., November 2, 1959.

REFERENCES

1. Finch, Thomas W., and Matranga, Gene J.: Launch, Low-Speed and Landing Characteristics Determined From the First Flight of the North American X-15 Research Airplane. NASA TM X-195, 1959.

2. McKay, James M.: Measurements Obtained During the First Landing of the North American X-15 Research Airplane. NASA TM X-207, 1959.

3. Alford, William J., Jr., and Taylor, Robert T.: Aerodynamic Characteristics of the X-15/B-52 Combination. NASA MEMO 6-8-59L, 1959.

TABLE I.- PHYSICAL CHARACTERISTICS OF THE AIRPLANE

Wing:	
Airfoil section	NACA 66005 (Modified)
Total area (includes 94.98 sq ft covered by fuselage), sq ft	200
Span, ft	22.36
Mean aerodynamic chord, ft	10.27
Root chord, ft	14.91
Tip chord, ft	2.98
Taper ratio	0.20
Aspect ratio	2.50
Sweep at 25-percent-chord line, deg	25.64
Incidence, deg	0
Dihedral, deg	0
Aerodynamic twist, deg	0
Flap -	
Type	Plain
Area (each), sq ft	8.30
Span (each), ft	4.50
Inboard chord, ft	2.61
Outboard chord, ft	1.08
Deflection, down, deg	40
Ratio flap chord to wing chord	0.22
Ratio total flap area to wing area	0.08
Ratio flap span to wing semispan	0.40
Trailing-edge angle, deg	5.67
Sweepback angle of hinge line, deg	0
Horizontal tail:	
Airfoil section	NACA 66005 (Modified)
Total area (includes 63.29 sq ft covered by fuselage), sq ft	115.34
Span, ft	18.08
Mean aerodynamic chord, ft	7.05
Root chord, ft	10.22
Tip chord, ft	2.11
Taper ratio	0.21
Aspect ratio	2.83
Sweep at 25-percent-chord line, deg	45
Dihedral, deg	-15
Ratio horizontal-tail area to wing area	0.58
Movable surface area, sq ft	51.77
Deflection -	
Longitudinal, up, deg	15
Longitudinal, down, deg	35
Lateral differential (pilot authority), deg	±15
Lateral differential (autopilot authority), deg	±30
Control system	Irreversible hydraulic boost with artificial feel
Upper vertical tail:	
Airfoil section	10° single wedge
Total area, sq ft	40.91
Span, ft	4.58
Mean aerodynamic chord, ft	8.95

TABLE I.- PHYSICAL CHARACTERISTICS OF THE AIRPLANE - Concluded

Root chord, ft	10.21
Tip chord, ft	7.56
Taper ratio	0.74
Aspect ratio	0.51
Sweep at 25-percent-chord line, deg	23.41
Ratio vertical-tail area to wing area	0.20
Movable surface area, sq ft	26.45
Deflection, deg	±7.50
Sweepback of hinge line, deg	0
Control system	Irreversible hydraulic boost with artificial feel
Lower vertical tail:	
Airfoil section	10° single wedge
Total area, sq ft	34.41
Span, ft	3.83
Mean aerodynamic chord, ft	9.17
Root chord, ft	10.21
Tip chord, ft	8
Taper ratio	0.78
Aspect ratio	0.43
Sweep at 25-percent-chord line, deg	23.41
Ratio vertical-tail area to wing area	0.17
Movable surface area, sq ft	19.95
Deflection, deg	±7.50
Sweepback of hinge line, deg	0
Control system	Irreversible hydraulic boost with artificial feel
Fuselage:	
Length, ft	50.75
Maximum width, ft	7.33
Maximum depth, ft	4.67
Maximum depth over canopy, ft	4.97
Side area (total), sq ft	215.66
Fineness ratio	10.91
Speed brake:	
Area (each), sq ft	5.57
Span (each), ft	1.67
Chord (each), ft	3.33
Deflection, deg	35

	Launch	Landing
Weight, lb	32,700	14,000
Center-of-gravity location, percent mean aerodynamic chord	20 1/2	19 1/2
Moments of inertia:		
I_X, slug-ft^2	5,100	3,600
I_Y, slug-ft^2	107,600	83,500
I_Z, slug-ft^2	109,300	85,100
I_{XZ}, slug-ft^2	-1,100	-500

TABLE II.- LONGITUDINAL CHARACTERISTICS

M	h_p, ft	α, deg	P, sec	$T_{1/2}$, sec	ξ (Damper effects included)	Derivatives from pulsed flight data (Damper effects included)		
						C_{N_α}, per deg	C_{m_α}, per deg	$C_{m_{\delta_h}}$, per deg
0.96	46,490	4.55	2.11	0.75	0.30	0.087	-0.039	-0.0233
1.166	46,330	5.5	2.1	.75	.30	.065	-.031	-.0287

TABLE III.- LATERAL CHARACTERISTICS

M	h_p, ft	α, deg	P, sec	$T_{1/2}$, sec	ξ (Damper effects included)	Derivatives from pulsed flight data (Damper effects included)		
						C_{n_β}, per deg	C_{l_β}, per deg	$C_{n_{\delta_v}}$, per deg
0.96	47,540	4.55	3.00	1.64	0.20	0.0094	0.00029	-0.0050
1.238	48,120	5.5	1.80	0.93	.21	.016	-.00139	-.0068
1.787	50,530	2.2	1.51	0.75	.21	.0115	-.00026	-.0055

TABLE IV.- ROLL-CONTROL EFFECTIVENESS

M	h_p, ft	α, deg	$C_{l_{\delta_a}}$, per deg
0.96	46,500	4.61	0.0035
1.166	46,300	5.10	.0019
1.869	49,330	2.32	.0014

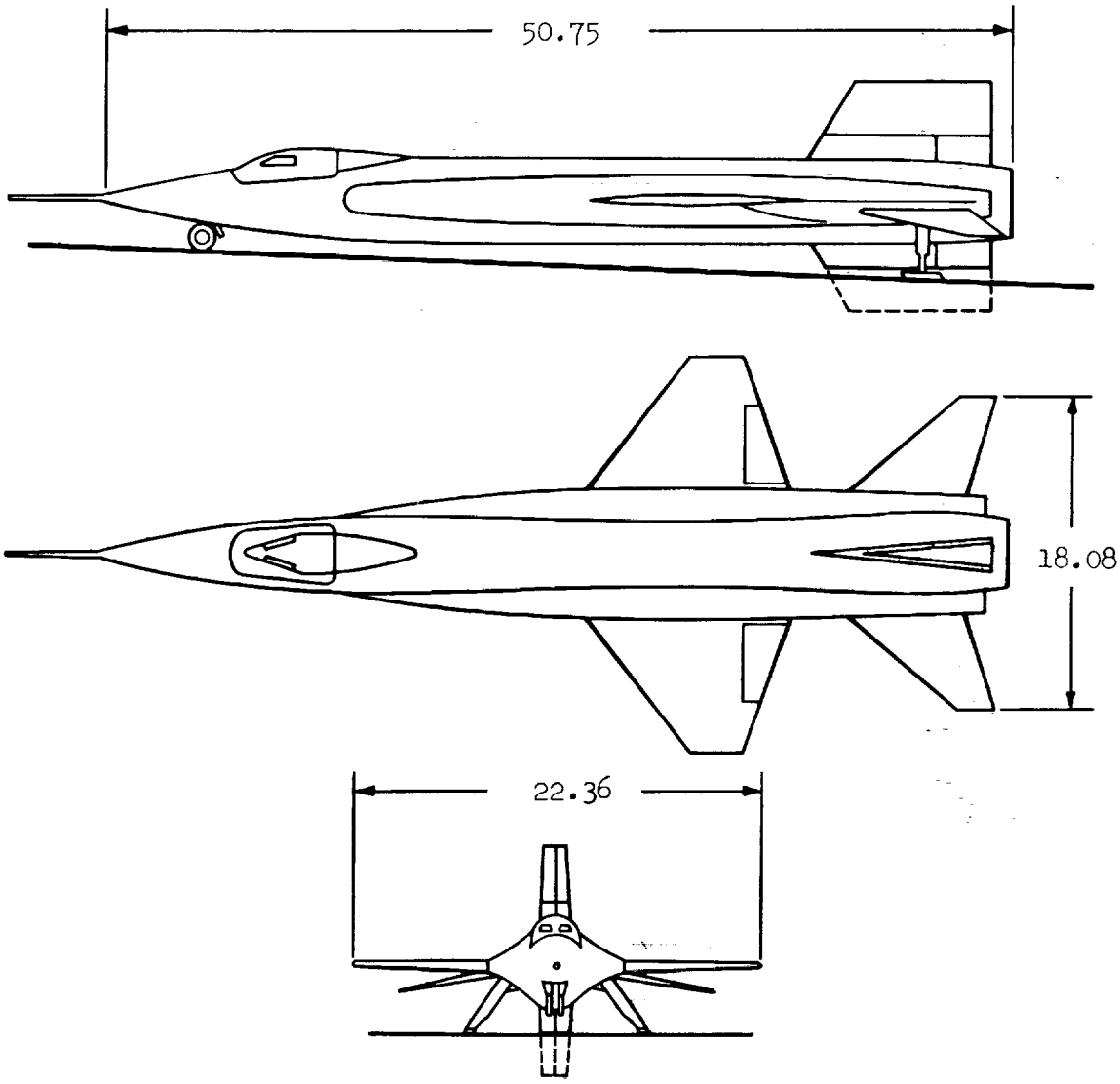

Figure 1.- Three-view drawing of the test airplane. All dimensions in feet.

Figure 2.- Photograph of the airplane. E-4484

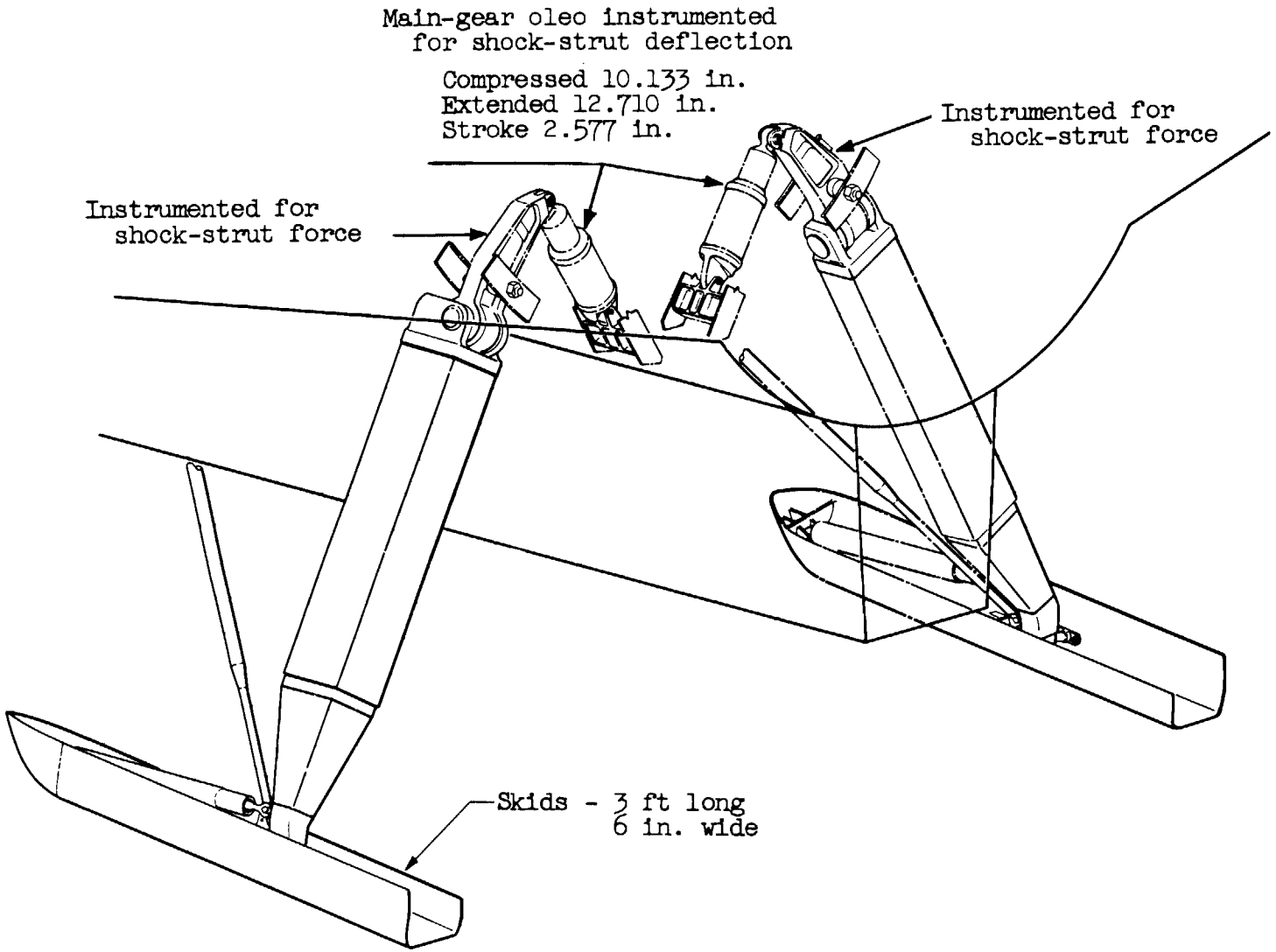

Figure 3.- Schematic drawing of the X-15 landing gear.

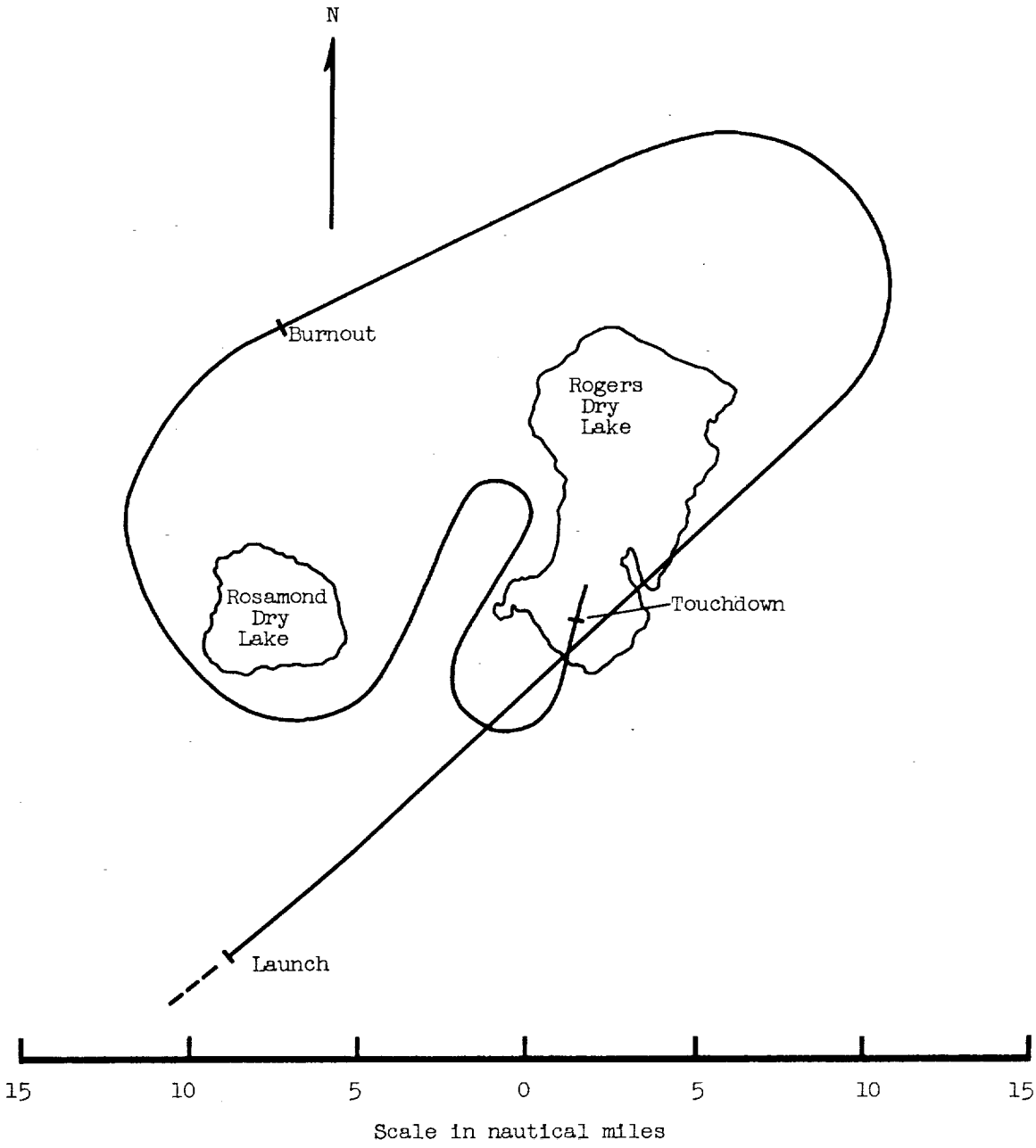

Figure 4.- General flight plan for first X-15 powered flight.

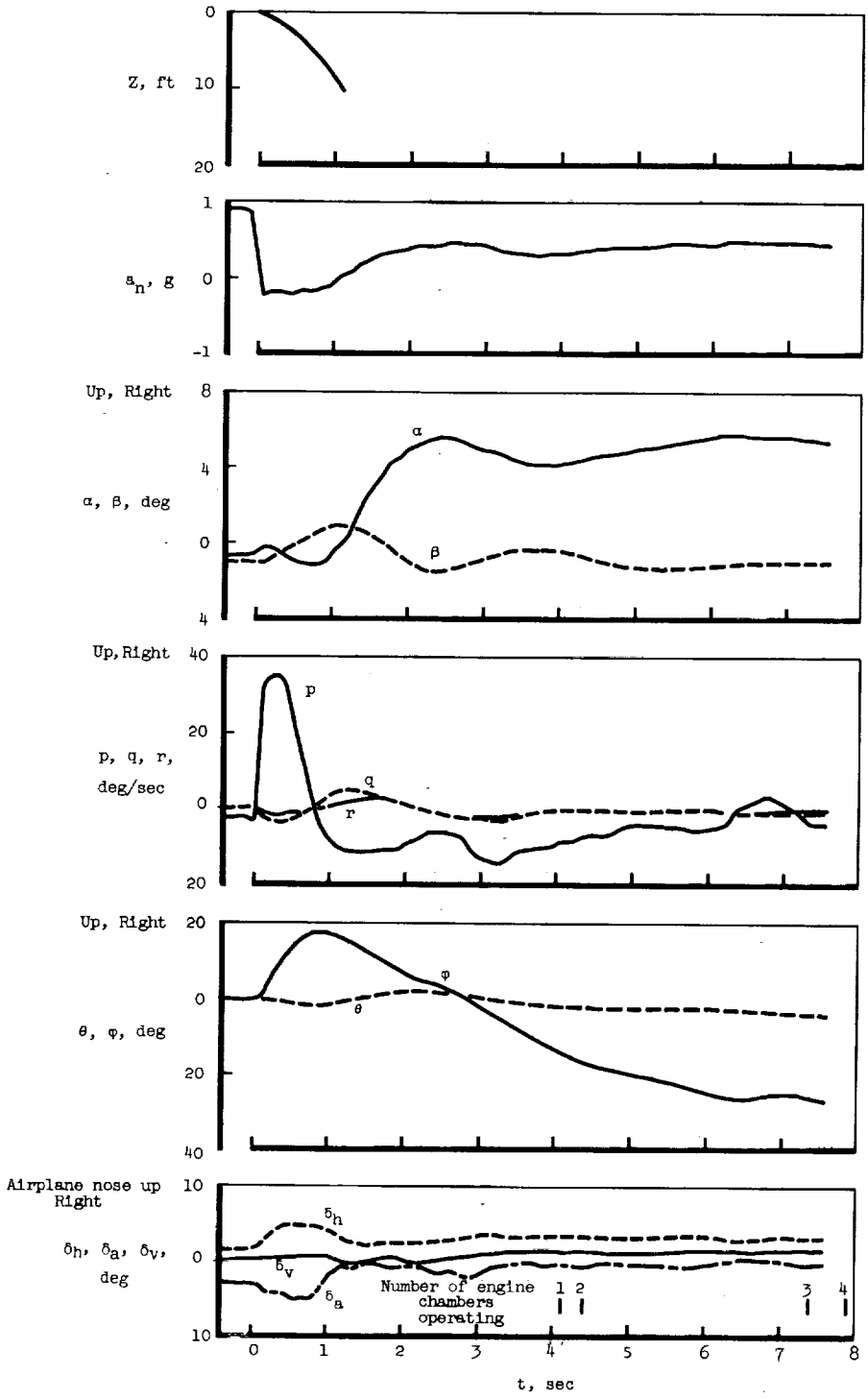

Figure 5.- Time history of the launch.

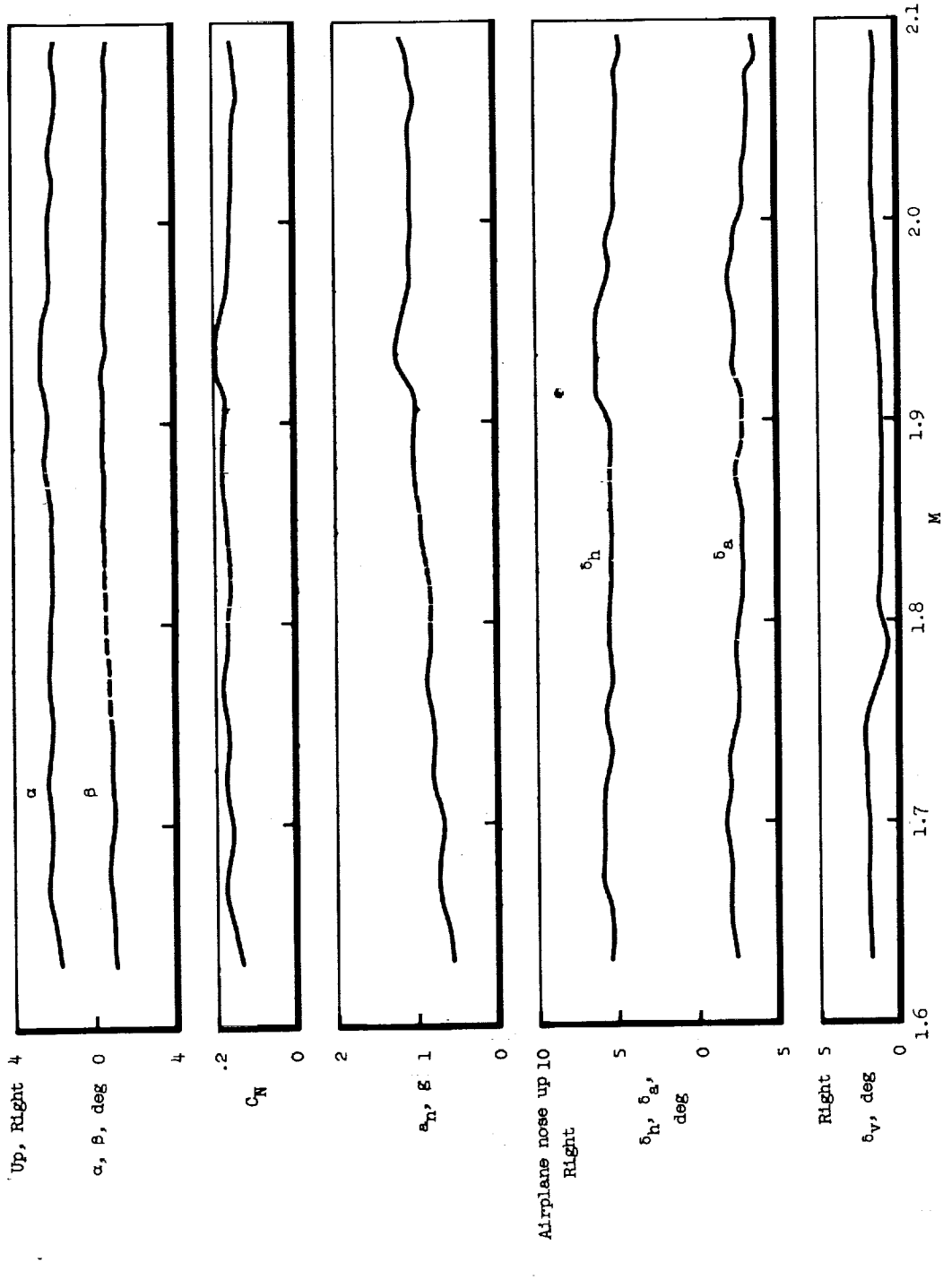

Figure 6.- Airplane trim characteristics during acceleration run. (Regions in which data were faired are shown by dashed lines.)

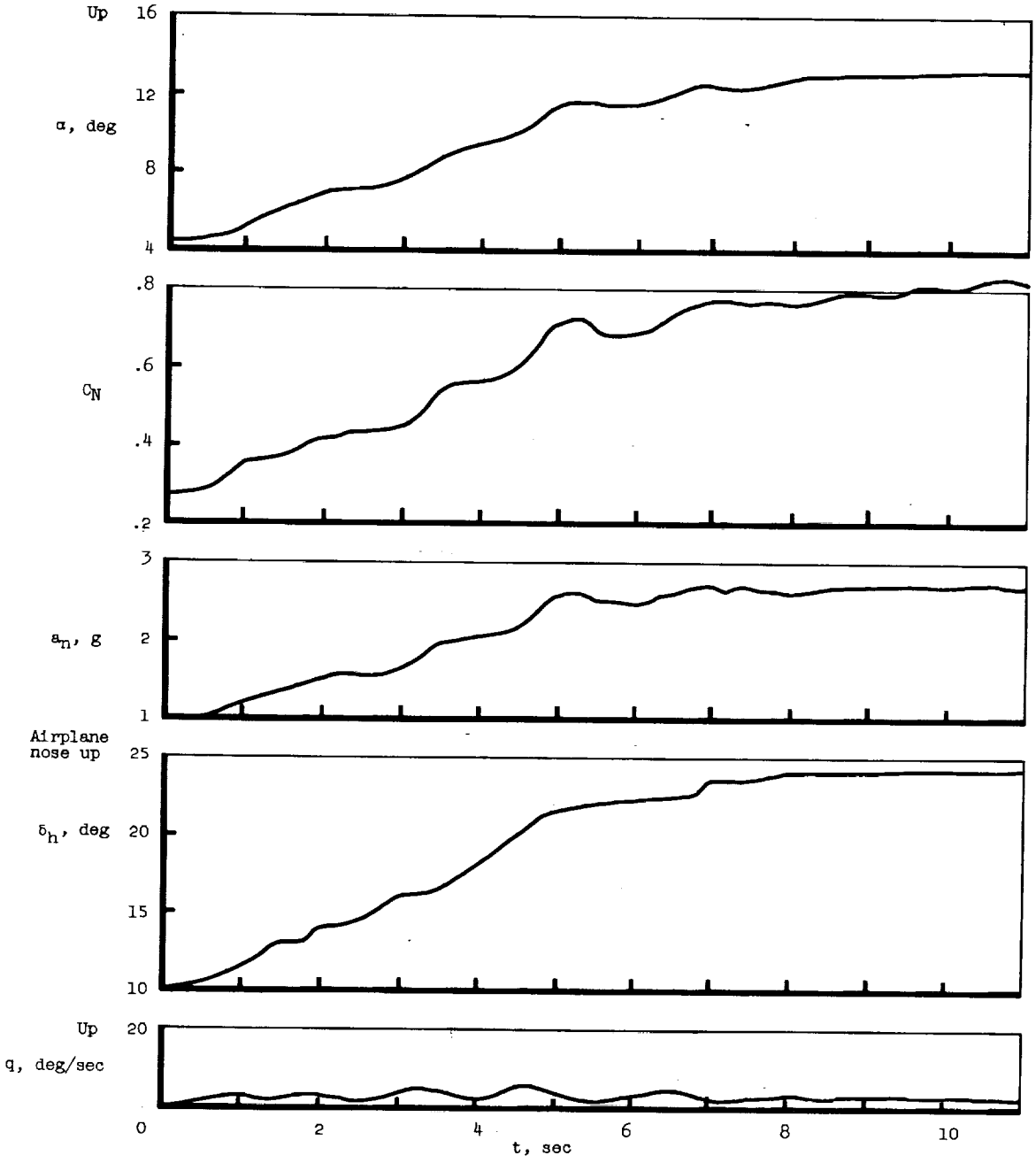

(a) M = 1.56; h_p = 48,000 feet.

Figure 7.- Time history of turn maneuvers.

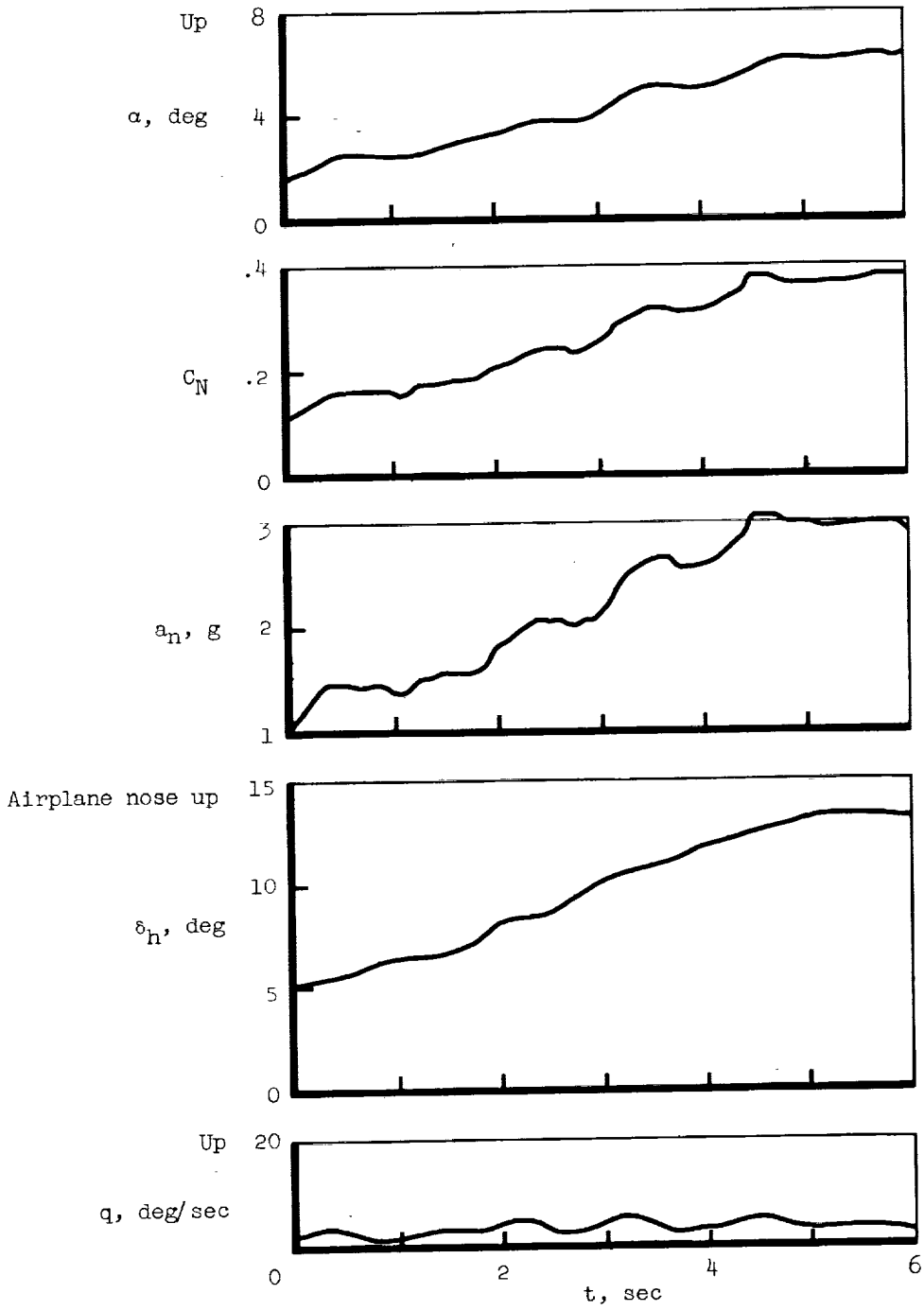

(b) M = 2.00; h_p = 47,000 feet.

Figure 7.- Concluded.

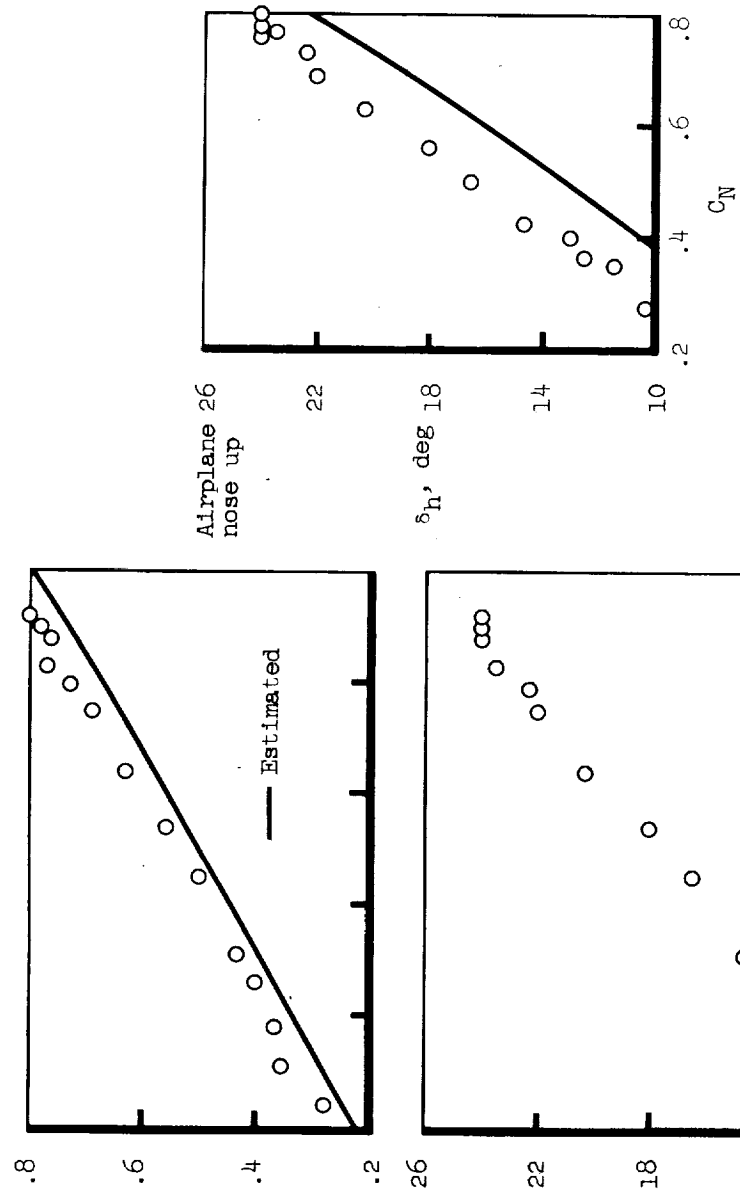

(a) M = 1.56; h_p = 48,000 feet.

Figure 8.- Longitudinal stability characteristics of the X-15 airplane determined during turn maneuvers.

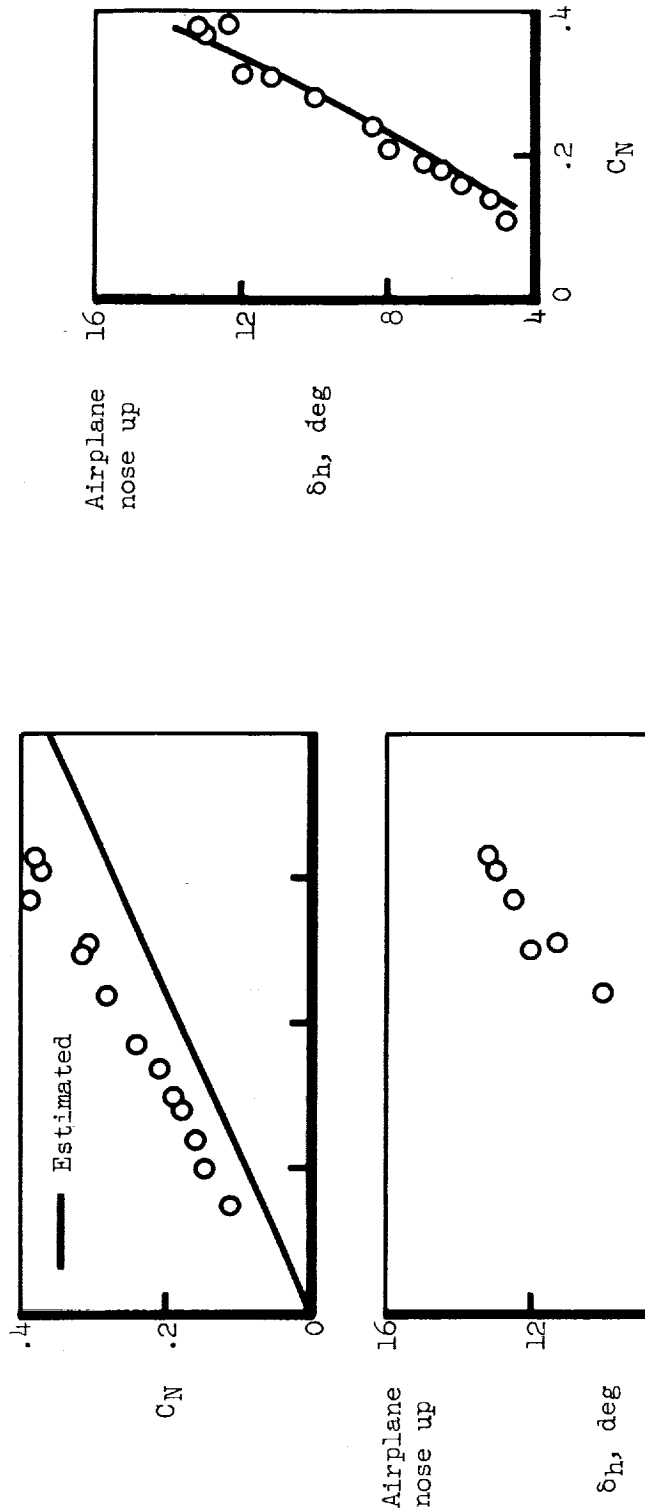

(b) M = 2.00; h_p = 47,000 feet.

Figure 8.- Concluded.

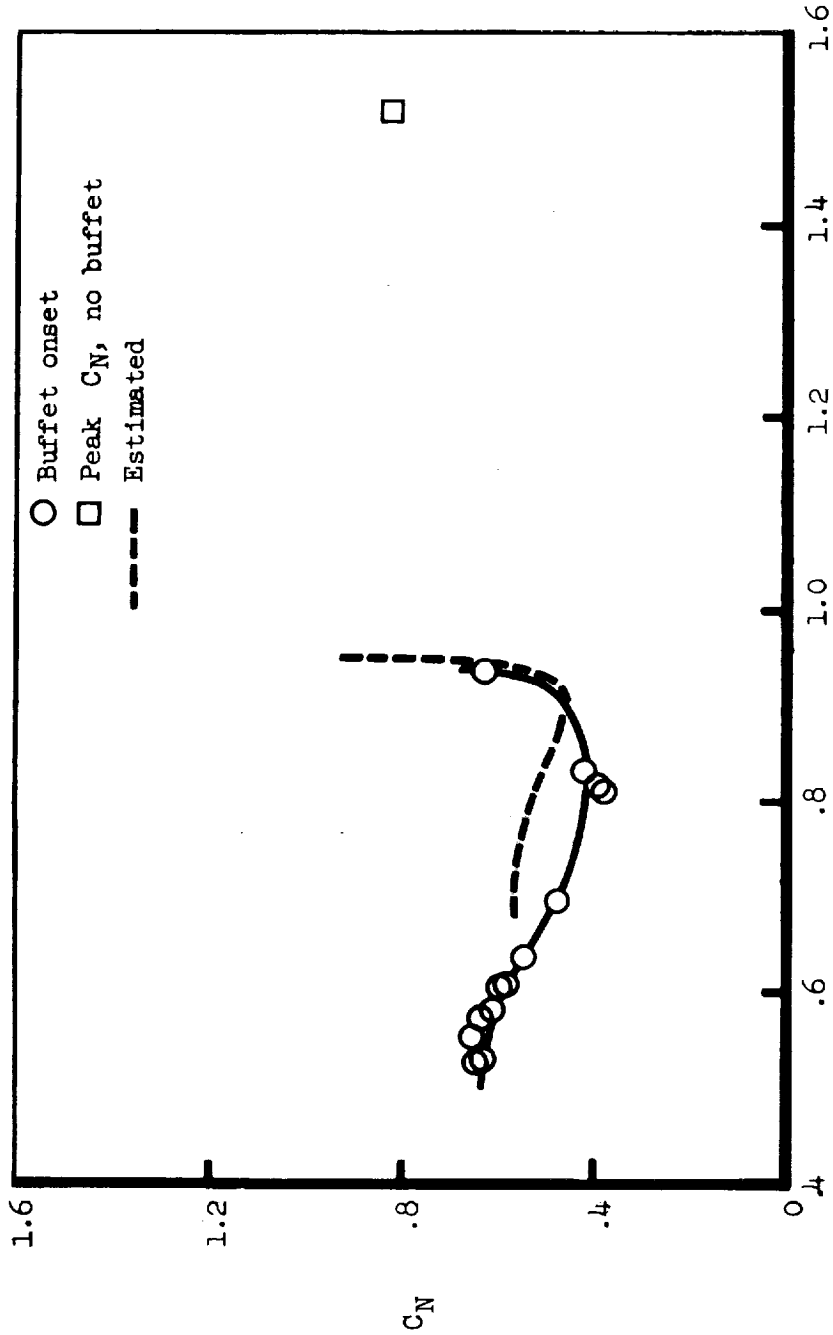

Figure 9.- Boundary for onset of buffet for X-15 airplane.

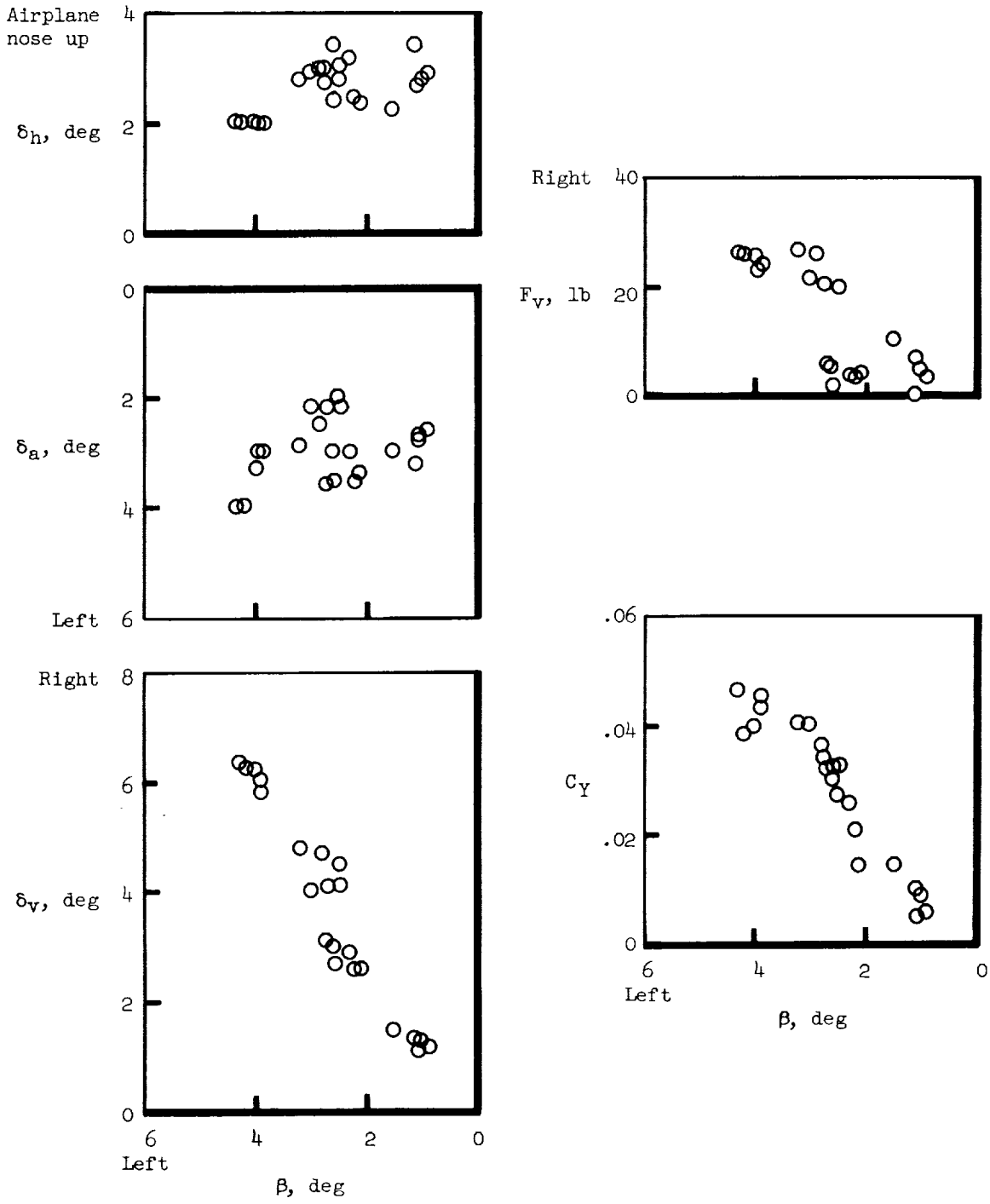

Figure 10.- Sideslip characteristics of the X-15 airplane. M = 0.95; h_p = 43,000 feet.

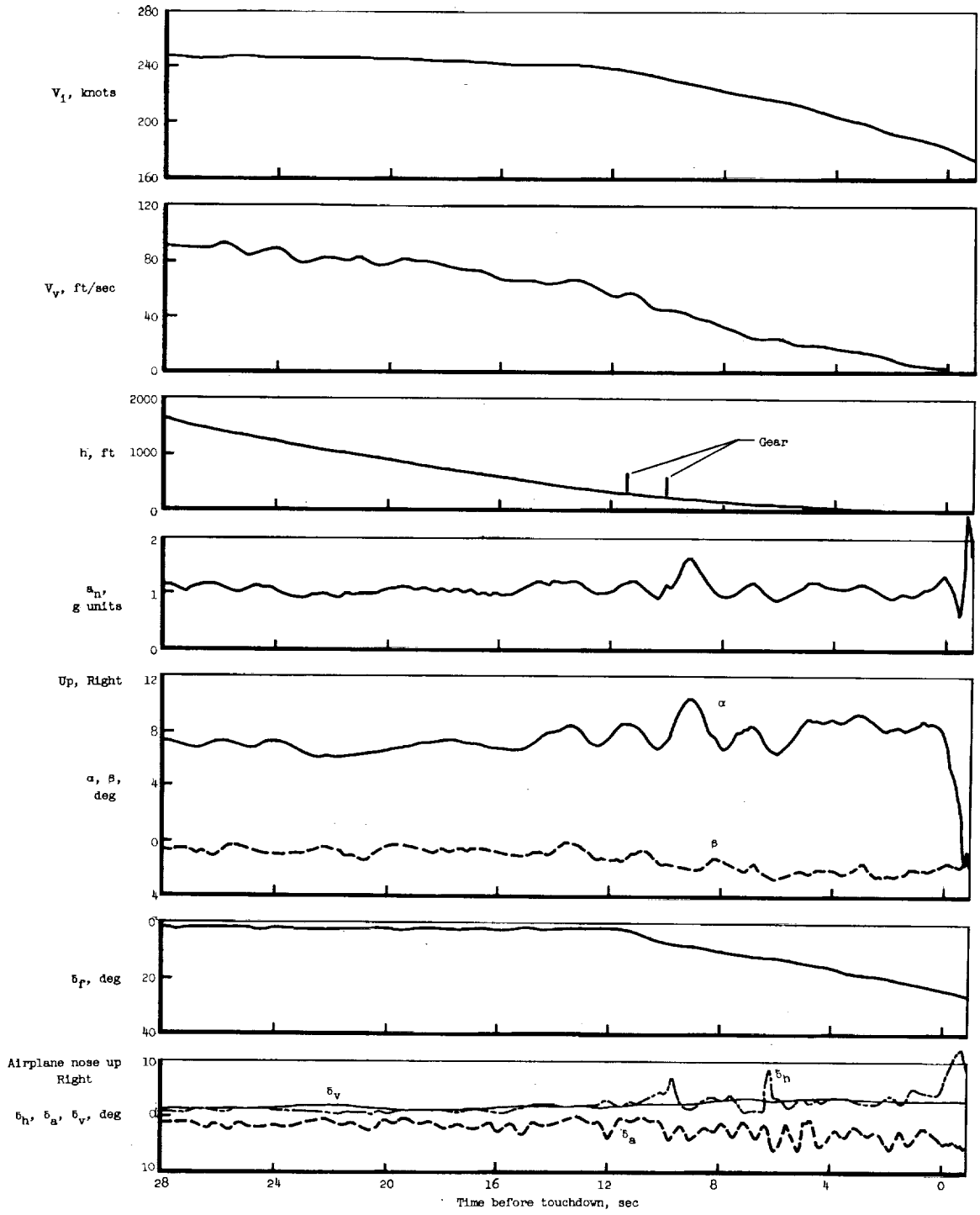

Figure 11.- Time history of final approach, flare, and touchdown.

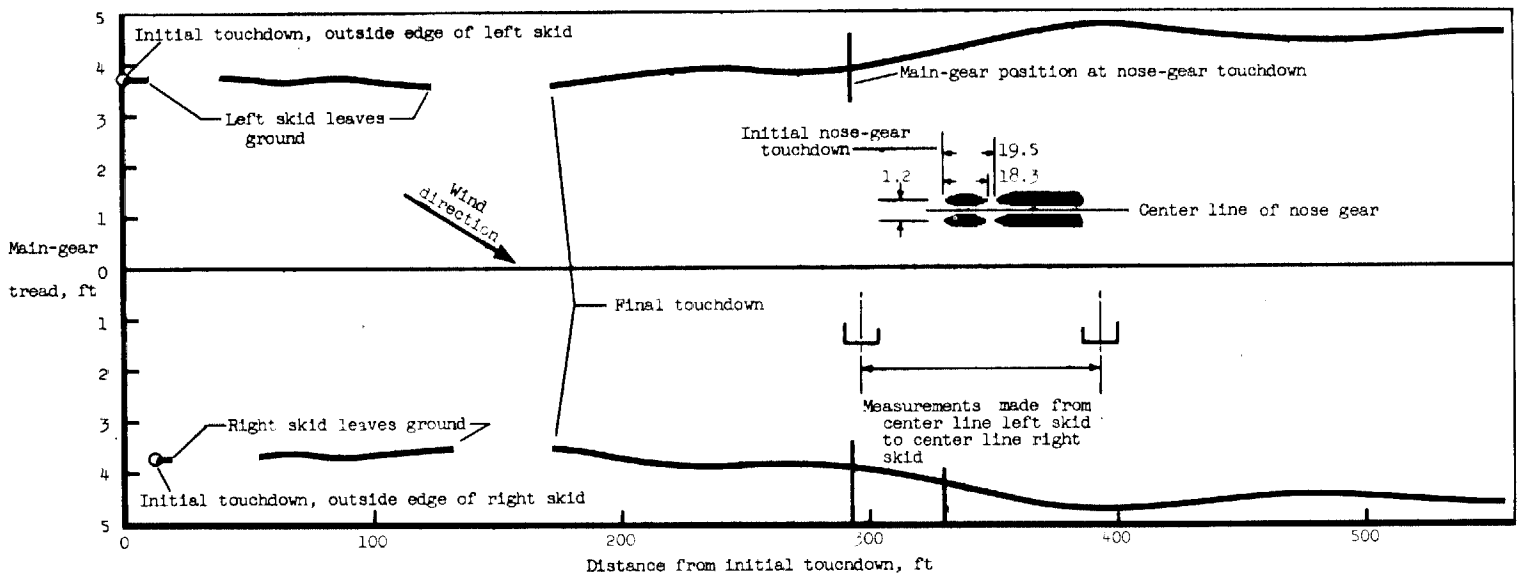

Figure 12.- Variation with distance down the runway from the initial touchdown point of the main-gear-tread distance during the landing of the X-15 airplane.

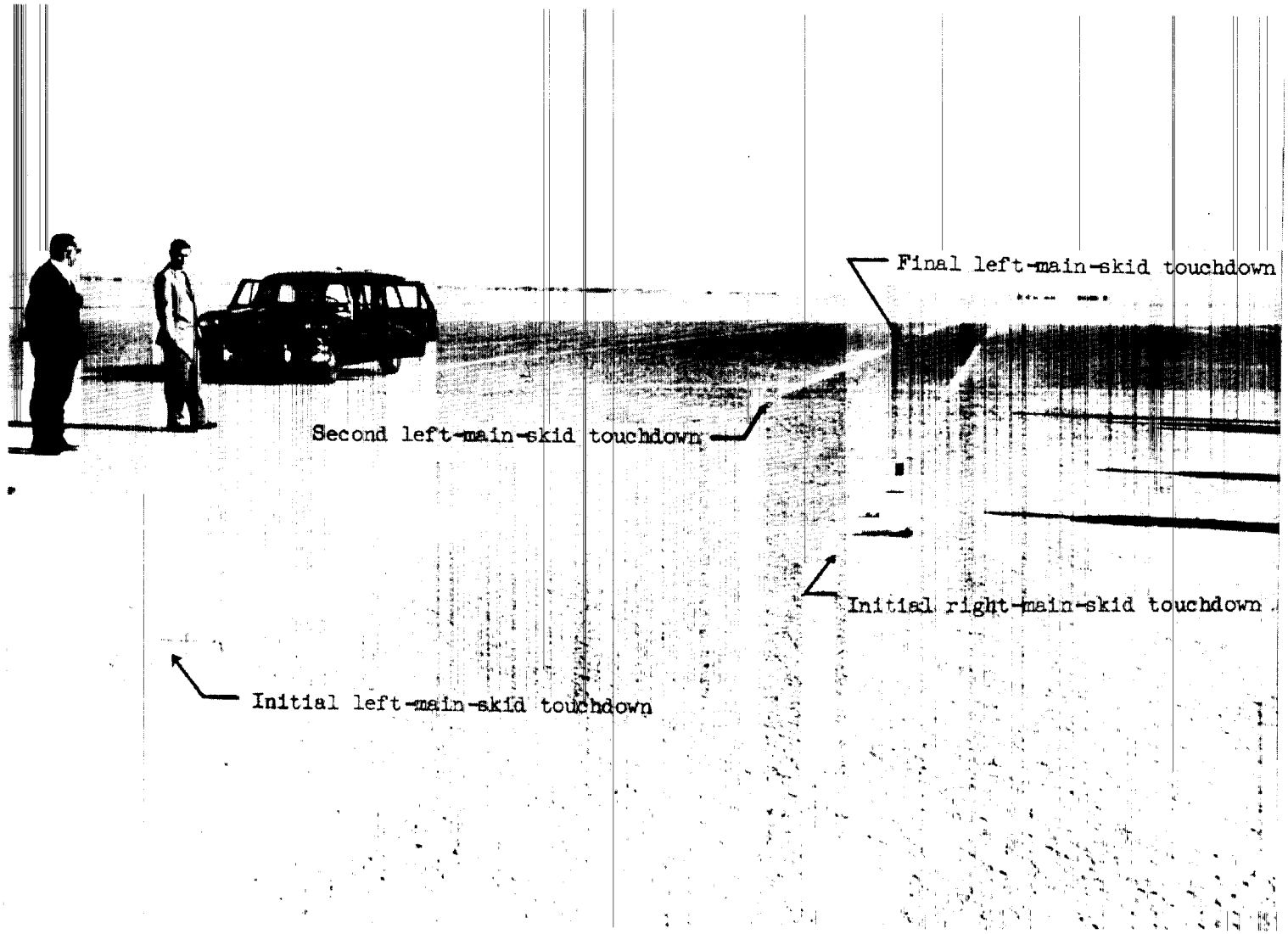

Figure 13.- Initial touchdown skid marks at landing. E-4980

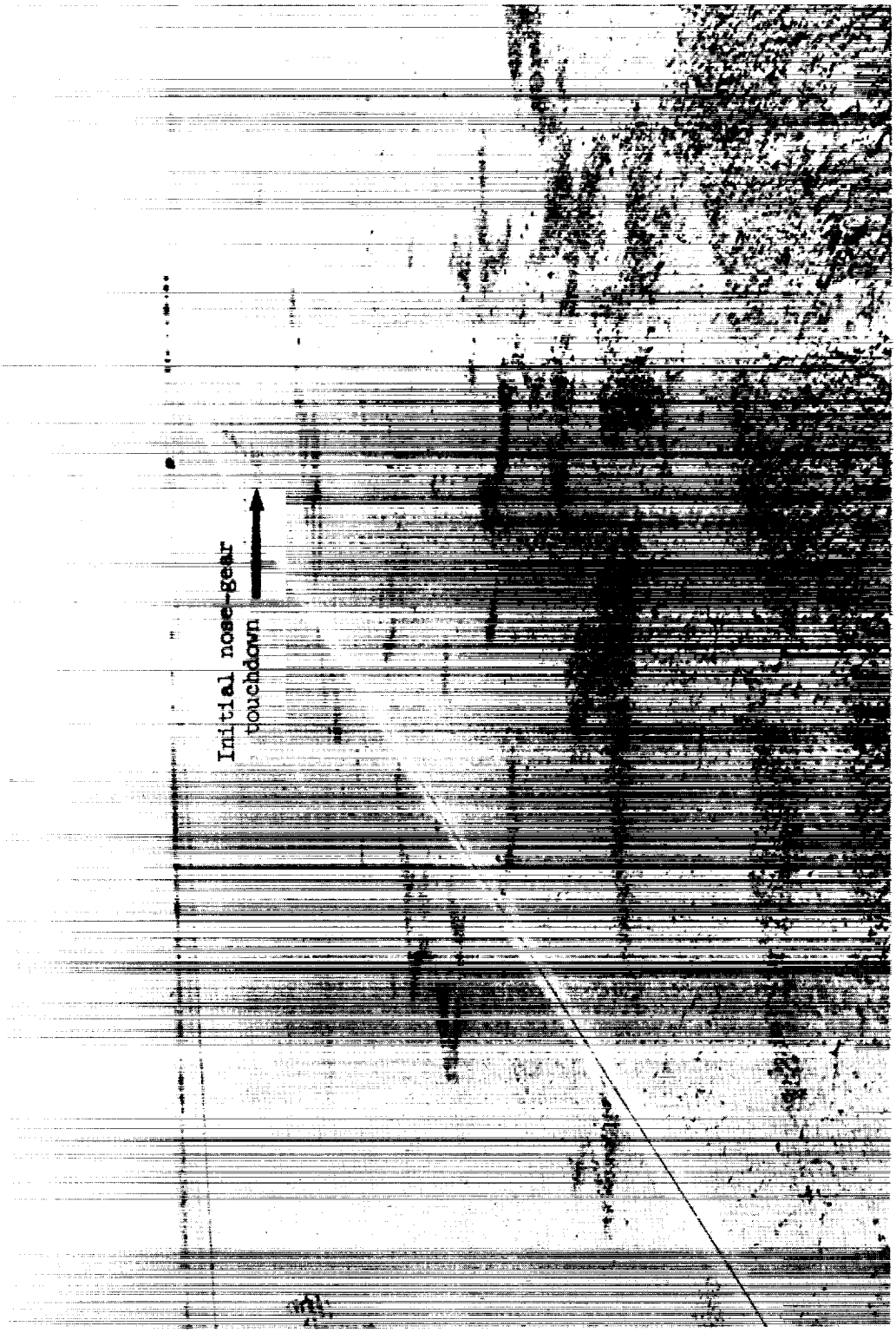

Figure 14.- Skid marks showing nose-gear touchdown. E-4981

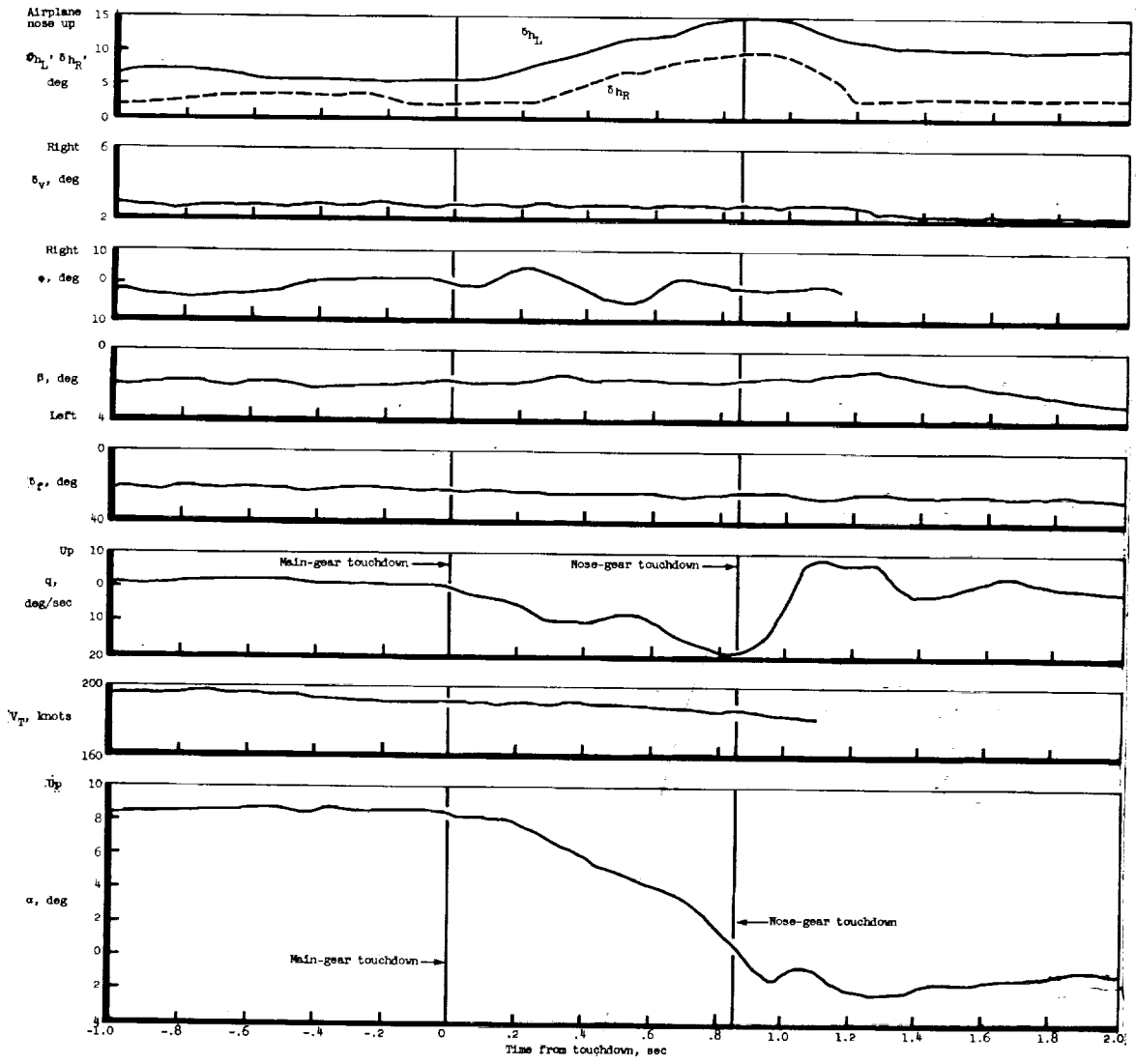

Figure 15.- Variation with time from touchdown of several airplane and aerodynamic quantities during the landing of the X-15 airplane.

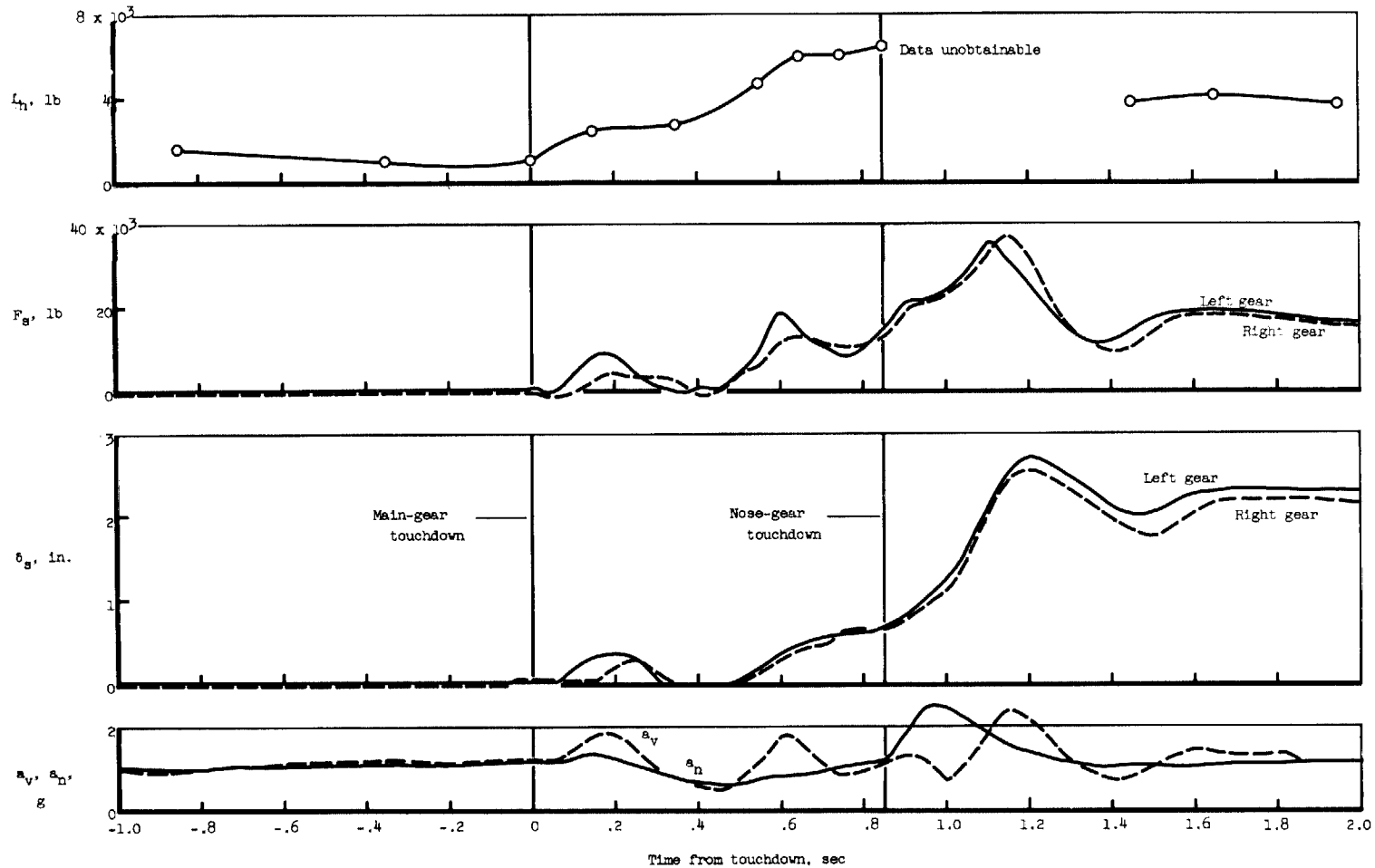

Figure 16.- Variation with time from touchdown of accelerations, main-gear shock-strut deflection and force, and horizontal-tail aerodynamic load during the landing of the X-15 airplane.

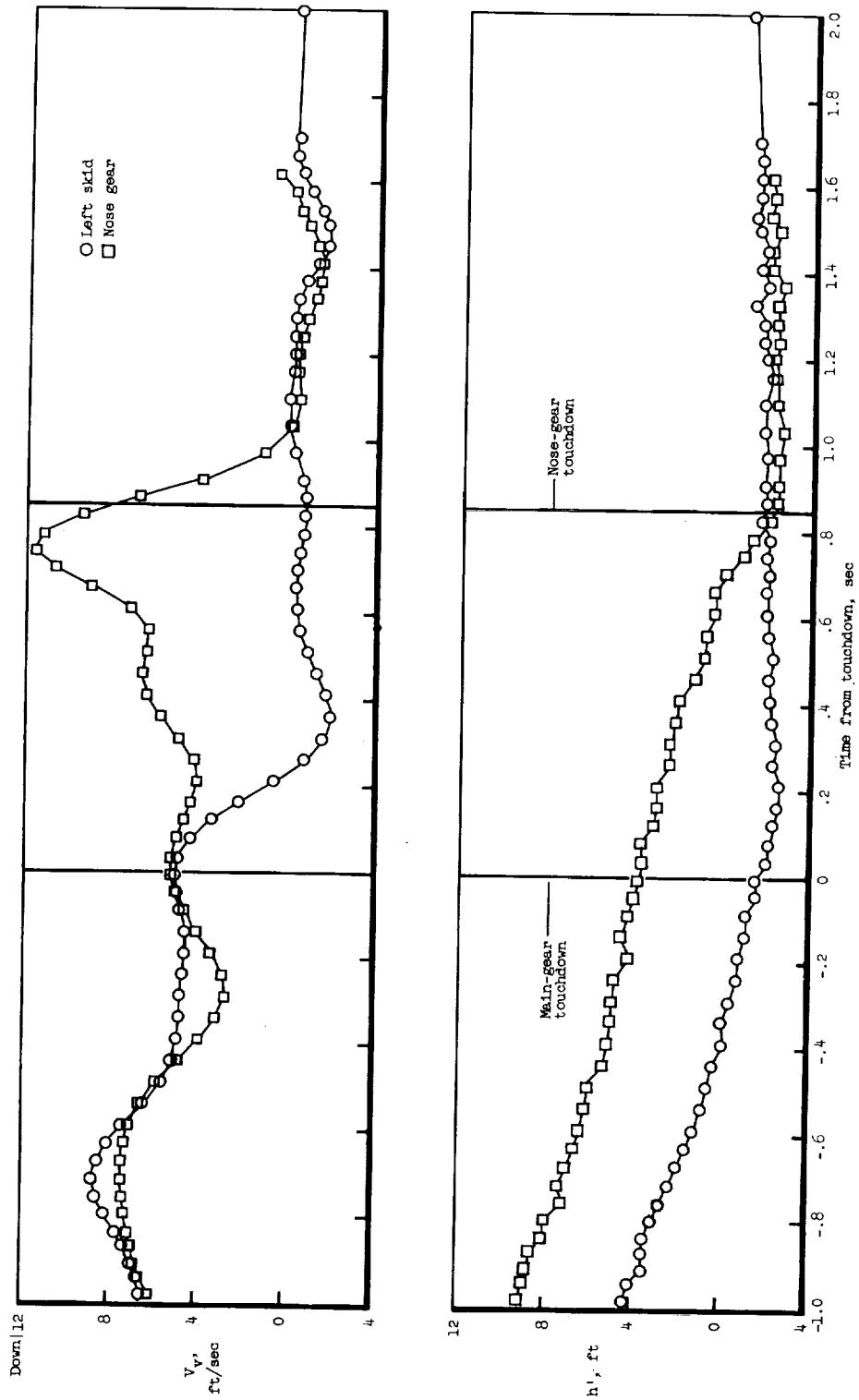

Figure 17.- Variation with time from touchdown of vertical velocity and height above reference plane for the main gear and nose gear during the landing of the X-15 airplane.

NASA - Langley Field, Va. H-151